Bayesian Detection for Radar Targets in Compound-Gaussian Sea Clutter

Jian Xue, Shuwen Xu, *Senior Member, IEEE*, Jun Liu, *Senior Member, IEEE*, Meiyan Pan, and Jie Fang

***Abstract*— We consider the detection problem of maritime radar targets in the training-sample-starved and non-Gaussian sea clutter environment. The performance of conventional detectors for radar targets is seriously degraded due to both the starvation of training samples for estimating the clutter covariance matrix and the non-Gaussianity of sea clutter. In this letter, we adopt the inverse Gaussian distribution and the inverse complex Wishart distribution to model the texture and speckle covariance matrix of sea clutter, respectively. Then an adaptive Bayesian detector is developed based on the two-step generalized likelihood ratio test and the maximum posterior estimates of clutter parameters. Finally, the experimental results on simulated and measured data demonstrate the performance superiority of the proposed detector over its competitors, especially when the training samples are starved.**

***Index Terms*— Adaptive detection, radar targets, sea clutter, training-sample-starved.**

I. Introduction

COMPLICATED and volatile characteristics of sea clutter have made the target detection of maritime radars receive considerable attention. Existence of both non-Gaussianity and non-homogeneity of sea clutter in practice leads to performance degradation of traditional detectors. Non-Gaussianity means that the probability of occurrence of sea spikes increases, and non-homogeneity makes the training samples for estimating the clutter covariance matrix starved. To enhance the detection performance of maritime radars in a training-sample-starved and non-Gaussian sea clutter environment, it is of crucial importance to take advantage of suitable statistical models for sea clutter.

The statistical characteristics of sea clutter amplitude play an important role in the design of adaptive coherent detectors. Non-Gaussian sea clutter usually represents the heavier-tailed behavior than the conventional Gaussian clutter [1]. The compound-Gaussian (CG) model can characterize the non-Gaussian sea clutter well from the standpoint of physical scattering and mathematical tractability [2]. Non-Gaussian sea clutter can be mathematically expressed by the product of a complex Gaussian process with zero mean (referred to as speckle) and a random positive texture component on the basis of the CG model. The texture component controls the sea clutter power, so the spatial and temporal changes of clutter texture will cause the power picture of sea clutter to exhibit the obvious bright and dark areas. Different distributions of the CG sea clutter can be derived via considering different distributions of clutter texture. The commonly used distributions are the K distribution with Gamma texture [3], the generalized Pareto (GP) distribution with inverse Gamma texture [4], and the CG distribution with inverse Gaussian (CG-IG) texture [5], [6]. Compared with the K and GP distributions, the CG-IG distribution can fit the real sea clutter best in some cases [6]. Actually, the texture distribution contains a clutter power parameter and a clutter non-Gaussian parameter. Thus, the texture distribution can be applied in the design of detectors for suppressing the CG sea clutter.

Besides statistically modeling of clutter texture, the speckle covariance matrix of CG sea clutter has to be estimated for whitening the correlated sea clutter in adaptive coherent detection. The training samples spatially surrounding the cell under test (CUT) are used to estimate the clutter/speckle covariance matrix. Three conventional estimators, the sample covariance matrix (SCM) [7], the normalized sample covariance matrix (NSCM) [8], and the constrained approximate maximum likelihood (CAML) [9], can perform well in the homogeneous sea clutter environment. However, in practical non-homogeneous clutter environments, adaptive coherent detectors using these estimators would suffer severe performance losses due to the starvation of training samples.

To improve the detection performance in the non-homogeneous sea clutter environment, the speckle covariance matrix can be regarded as a stochastic matrix, and then its prior distribution can be used to design detectors on account of Bayes' theorem. Besson *et al.* [10] proposed a detector for point-like targets in Gaussian clutter via using the prior distribution of the clutter covariance matrix, and numerical simulations show that the proposed detector outperforms the conventional adaptive matched filter. Several detectors without secondary data were proposed for distributed targets in the GP clutter, and they also perform satisfactory performance [11]. Kong *et al.* [12] studied the target detector for multiple-input multiple-output (MIMO) radars in the GP clutter, and the

Manuscript received October 24, 2021; revised December 7, 2021; accepted December 30, 2021. Date of publication January 6, 2022; date of current version January 20, 2022. This work was supported in part by the National Natural Science Foundation of China under Grant 61871303, Grant 61871469, and Grant 61771442; in part by the Foreign Scholars in University Research and Teaching Programs through the 111 Project; in part by the Youth Innovation Promotion Association CAS under Grant CX2100060053; in part by the USTC Tang Scholar; and in part by the Key Research Program of the Frontier Sciences, CAS, under Grant QYZDY-SSW-JSC035. *(Corresponding authors: Jian Xue; Shuwen Xu.)*

Jian Xue and Jie Fang are with the School of Communications and Information Engineering, Xi'an University of Posts and Telecommunications, Xi'an 710021, China (e-mail: jxue@xupt.edu.cn).

Shuwen Xu is with the National Laboratory of Radar Signal Processing, Xidian University, Xi'an 710071, China (e-mail: swxu@mail.xidian.edu.cn).

Jun Liu is with the Department of Electronic Engineering and Information Science, University of Science and Technology of China, Hefei 230026, China.

Meiyan Pan is with the Xi'an Electronic Engineering Research Institute, Xi'an 710071, China.

Digital Object Identifier 10.1109/LGRS.2022.3140727

proposed detectors outperform some existing detectors in training-limited scenarios due to the use of the prior distribution of the speckle covariance matrix. Range-spread target detection for distributed MIMO radars was investigated in [13], and the prior distribution of the speckle covariance matrix improves the detection performance for radar targets. A detector, referred to as the Bayesian generalized likelihood ratio test detector without secondary data (BGLRTD-NSD) here, was proposed for improving the detection performance in the CG-IG sea clutter background [14]. BGLRTD-NSD can perform well in the training-sample-starved scenario, whereas its performance is inferior to its competitor (the generalized likelihood ratio test with inverse Gaussian texture, GLRT-IG [15]) when the training samples become sufficient.

The prior knowledge about clutter can be used to enhance the performance of clutter suppression and target detection [16]. Therefore, we focus on designing an adaptive coherent detector using the clutter prior knowledge in the non-homogeneous CG-IG sea clutter environment. Different from BGLRTD-NSD, we aim to make the designed detector adapt to the change in not only non-Gaussianity but also inhomogeneity of sea clutter. The inverse Gaussian distribution is used to model the CG clutter texture, and the inverse complex Wishart distribution is adopted to characterize the speckle covariance matrix. The prior distributions of the clutter texture and the speckle covariance matrix are jointly used at the design stage. Then, according to the two-step generalized likelihood ratio test (2S-GLRT) and the maximum *a posteriori* (MAP) estimate, we propose an adaptive coherent detector. Moreover, an iterative estimator for the speckle covariance matrix is derived in the CG-IG sea clutter.

II. Detection Problem Description

Assume a coherent radar successively transmits N pulses. The CUT contains an N-dimensional complex vector $\boldsymbol{z} = [z(1), z(2), \ldots, z(N)]^{\mathrm{T}}$, where $(\cdot)^{\mathrm{T}}$ denotes the transpose operation. Meanwhile, the training samples from K range cells, $\boldsymbol{z}_k = [z_k(1), z_k(2), \ldots, z_k(N)]^{\mathrm{T}}$, $k = 1, 2, \ldots, K$, are assumed to be available for estimating the speckle covariance matrix. The detection problem of radar targets in the sea-clutter-dominated environment can be formulated in terms of the following binary hypotheses test:

$$\begin{cases} \mathrm{H}_0: \begin{cases} \boldsymbol{z} = \boldsymbol{c} \\ \boldsymbol{z}_k = \boldsymbol{c}_k, \quad k = 1, 2, \ldots, K \end{cases} \\ \mathrm{H}_1: \begin{cases} \boldsymbol{z} = \alpha \boldsymbol{p} + \boldsymbol{c} \\ \boldsymbol{z}_k = \boldsymbol{c}_k, \quad k = 1, 2, \ldots, K \end{cases} \end{cases} \tag{1}$$

where H_0 denotes that the target is absent, H_1 means that the target is present, α is the target amplitude, $\boldsymbol{p} = [1, e^{j2\pi f_d}, \ldots, e^{j2\pi(N-1)f_d}]^{\mathrm{T}}$ is the target steering vector, and f_d denotes the normalized target Doppler frequency.

In a radar coherent process interval (CPI), the CG sea clutter can be modeled as

$$\boldsymbol{c} = \sqrt{\tau}\boldsymbol{u}, \quad \boldsymbol{c}_k = \sqrt{\tau_k}\boldsymbol{u}_k, \quad k = 1, 2, \ldots, K \tag{2}$$

where τ (or τ_k) denotes the texture component, and $\boldsymbol{u}$ (or $\boldsymbol{u}_k$) denotes the speckle component. The clutter vectors $\boldsymbol{c}$ and $\boldsymbol{c}_k$ are assumed to be independent and distributed. In this letter, the texture τ is considered to obey the inverse Gaussian distribution, and its probability density function (PDF) is given by

$$f(\tau; \eta, \mu) = \sqrt{\frac{\mu\eta}{2\pi}}\tau^{-3/2}\exp\left(-\frac{\eta(\tau-\mu)^2}{2\mu\tau}\right) \tag{3}$$

where η is the shape parameter, and μ is the scale parameter. The speckle $\boldsymbol{u}$ in (2) is an N-dimensional complex Gaussian vector with a zero mean and an $N \times N$-dimensional covariance matrix $\boldsymbol{R} = E(\boldsymbol{u}\boldsymbol{u}^H)$, where $E(\cdot)$ denotes the statistical expectation and $(\cdot)^H$ denotes the conjugate transpose. We consider the speckle covariance matrix $\boldsymbol{R}$ as a stochastic matrix following the inverse complex Wishart distribution given by [11] and [17]:

$$f(\boldsymbol{R}) = \frac{|\boldsymbol{R}|^{-(\upsilon+N)}|\upsilon\boldsymbol{\Sigma}|^{\upsilon}\mathrm{etr}\{-\upsilon\boldsymbol{R}^{-1}\boldsymbol{\Sigma}\}}{\pi^{N(N-1)/2}\prod_{i=1}^{N}\Gamma(\upsilon-i+1)} \tag{4}$$

where $\mathrm{etr}\{\cdot\}$ denotes the exponential of the trace of a matrix, $|\cdot|$ denotes the determinant of the matrix argument, υ is the degrees of freedom, $\boldsymbol{\Sigma}$ is a positive definite matrix, and $\Gamma(\cdot)$ is the Eulerian Gamma function.

Based on the clutter model in (2), the conditional PDFs of $\boldsymbol{z}$ can be given under the H_0 and H_1 hypotheses as follows:

$$f(\boldsymbol{z}|\boldsymbol{R}, \tau; H_0) = \frac{1}{(\pi\tau)^N|\boldsymbol{R}|}\mathrm{etr}\left\{-\frac{\boldsymbol{R}^{-1}\boldsymbol{z}\boldsymbol{z}^H}{\tau}\right\} \tag{5}$$

and

$$f(\boldsymbol{z}|\alpha, \boldsymbol{R}, \tau; H_1) = \frac{\mathrm{etr}\left\{-\frac{\boldsymbol{R}^{-1}(\boldsymbol{z}-\alpha\boldsymbol{p})(\boldsymbol{z}-\alpha\boldsymbol{p})^H}{\tau}\right\}}{(\pi\tau)^N|\boldsymbol{R}|}. \tag{6}$$

The detection problem of radar targets in CG-IG clutter environments has been investigated in [14] and [15]. GLRT-IG in [15] requires a large number of training samples to estimate the speckle covariance matrix, so it suffers much performance losses when the training samples are starved. BGLRTD-NSD in [14] can work well in training-sample-starved CG-IG clutter environments, whereas its performance cannot be improved as the number of training samples increases. In this letter, we focus on developing an adaptive Bayesian detector for radar targets in CG-IG clutter, and the designed detector can perform well for different numbers of training samples.

III. Adaptive Coherent Detector Design

In this section, an adaptive Bayesian detector is developed for radar targets in sea clutter on the basis of 2S-GLRT.

A. Detector Design With a Known Covariance Matrix

Assuming that $\boldsymbol{R}$ is known first, 2S-GLRT can be written as

$$\frac{\max_{\alpha,\tau} f(\boldsymbol{z}|\alpha, \boldsymbol{R}, \tau; H_1)f(\tau)}{\max_{\tau} f(\boldsymbol{z}|\boldsymbol{R}, \tau; H_0)f(\tau)} = \frac{\max_{\alpha,\tau}\tau^{-(N+3/2)}\exp\left\{-\left[\frac{\eta\tau}{2\mu}+\frac{\mu\eta/2+\tilde{q}_1}{\tau}\right]\right\}}{\max_{\tau}\tau^{-(N+3/2)}\exp\left\{-\left[\frac{\eta\tau}{2\mu}+\frac{\mu\eta/2+\tilde{q}_0}{\tau}\right]\right\}} \underset{H_0}{\overset{H_1}{\gtrless}} \gamma \tag{7}$$

where $\tilde{q}_0 = z^H \boldsymbol{R}^{-1} z$, $\tilde{q}_1 = (z - \alpha \boldsymbol{p})^H \boldsymbol{R}^{-1}(z - \alpha \boldsymbol{p})$, and γ is the detection threshold.

The maximum likelihood estimate (MLE) of α can be given by

$$\hat{\alpha} = \frac{\boldsymbol{p}^H \boldsymbol{R}^{-1} z}{\boldsymbol{p}^H \boldsymbol{R}^{-1} \boldsymbol{p}}. \tag{8}$$

Next, we calculate the MAP estimate of τ under the H_1 hypothesis. For a given $\hat{\alpha}$, the posteriori distribution of τ can be derived as

$$\begin{aligned} f(\tau|\hat{\alpha}, \boldsymbol{R}, z; H_1) &\propto f(z|\hat{\alpha}, \boldsymbol{R}, \tau; H_1) f(\tau) \\ &\propto \tau^{-(3/2+N)} \exp\left\{ -\left[\frac{\eta\tau}{2\mu} + \frac{\hat{q}_1}{\tau} \right] \right\} \end{aligned} \tag{9}$$

where

$$\begin{aligned} \hat{q}_1 &= \mu\eta/2 + (z - \hat{\alpha}\boldsymbol{p})^H \boldsymbol{R}^{-1}(z - \hat{\alpha}\boldsymbol{p}) \\ &= \mu\eta/2 + z^H \boldsymbol{R}^{-1} z - \frac{\left| \boldsymbol{p}^H \boldsymbol{R}^{-1} z \right|^2}{\boldsymbol{p}^H \boldsymbol{R}^{-1} \boldsymbol{p}}. \end{aligned} \tag{10}$$

For simplicity, taking the logarithm of (9), we have

$$\ln f(\tau|\hat{\alpha}, \boldsymbol{R}, z; H_1) = -(3/2 + N)\ln\tau - \frac{\eta\tau}{2\mu} - \frac{\hat{q}_1}{\tau}. \tag{11}$$

Differentiating (11) over τ and equating it to zero, the MAP estimate of τ is obtained as

$$\hat{\tau}_1 = \frac{\mu}{\eta}\left[-(N + 3/2) + \sqrt{(N + 3/2)^2 + \frac{2\eta}{\mu}\hat{q}_1} \right]. \tag{12}$$

Similarly, the MAP estimate of τ under the H_0 hypothesis can also be derived as

$$\hat{\tau}_0 = \frac{\mu}{\eta}\left[-(N + 3/2) + \sqrt{(N + 3/2)^2 + \frac{2\eta}{\mu}q_0} \right] \tag{13}$$

where $q_0 = \mu\eta/2 + z^H \boldsymbol{R}^{-1} z$.

Substituting (8), (12), and (13) into (7), a detector for radar targets can be given by

$$(N + 3/2)\ln\left(\frac{\hat{\tau}_0}{\hat{\tau}_1}\right) + \frac{\eta(\hat{\tau}_0 - \hat{\tau}_1)}{2\mu} + \frac{q_0}{\hat{\tau}_0} - \frac{\hat{q}_1}{\hat{\tau}_1} \underset{H_0}{\overset{H_1}{\gtrless}} \gamma' \tag{14}$$

where γ' is the modified detection threshold.

B. Estimation of the Speckle Covariance Matrix

To get the adaptive version of the detector (14), the second step in 2S-GLRT, which replaces $\boldsymbol{R}$ with its estimated value, is carried out. First, we tackle with the estimation problem of υ in (4). The precise prior information of υ is difficult to obtain, so we adopt the non-informative prior distribution to model it in this letter. The parameter υ is modeled as a uniform discrete random variable, i.e., $\upsilon \sim \mathrm{U}_{\upsilon_l,\ldots,\upsilon_u}$, where υ_l and υ_u are the integers determining the bounds of the estimation. The minimum mean square error (MMSE) estimate of υ in the k-th range cell of training samples can be derived by computing the conditional posterior distribution

$$\begin{aligned} f(\upsilon|z_k, \tau_k; H_j) &= \frac{\int f(z_k|\upsilon, \tau_k, \boldsymbol{R}; H_0) f(\boldsymbol{R}|\upsilon) f(\upsilon) d\boldsymbol{R}}{f(z_k|\tau_k)} \\ &= \bar{c}\frac{I_{\upsilon_l,\upsilon_u}(\upsilon)\left|\upsilon\boldsymbol{\Sigma}\right|^{\upsilon} \prod_{i=1}^{N} \upsilon - i + 1}{\left|\upsilon\boldsymbol{\Sigma} + \tau_k^{-1} z_k z_k^H\right|^{\upsilon+1}} \end{aligned} \tag{15}$$

where $I_{\upsilon_l,\upsilon_u}(\upsilon)$ is the indicator function, and $\bar{c}$ is a normalization factor. Thus, for a given τ_k, the MMSE estimate of υ in the k-th range cell can be calculated by

$$\hat{\upsilon}_k|\tau_k = \frac{\sum_{\upsilon=\upsilon_l}^{\upsilon_u} \upsilon h(\upsilon)}{\sum_{\upsilon=\upsilon_l}^{\upsilon_u} h(\upsilon)} \tag{16}$$

where

$$h(\upsilon) = \frac{\left|\upsilon\boldsymbol{\Sigma}\right|^{\upsilon} \prod_{i=1}^{N} \upsilon - i + 1}{\left|\upsilon\boldsymbol{\Sigma} + \tau^{-1} z_k z_k^H\right|^{\upsilon+1}}. \tag{17}$$

Replacing $\boldsymbol{R}$ with $\boldsymbol{\Sigma}$, the MLE of $\hat{\tau}_k^{\mathrm{MLE}}$ in (5) can be given by $\hat{\tau}_k^{\mathrm{MLE}} = 1/N z_k \boldsymbol{\Sigma}^{-1} z_k$. Therefore, for a given $\hat{\tau}_k^{\mathrm{MLE}}$, we can obtain $\hat{\upsilon}_k$. All the training samples share the same υ, so the estimate of υ can be calculated by $\hat{\upsilon} = 1/K \sum_{k=1}^{K} \upsilon_k$.

Next, the MAP estimate of $\boldsymbol{R}$ is addressed. The joint posterior PDF of $\boldsymbol{\tau} = [\tau_1, \tau_2, \ldots, \tau_K]$ and $\boldsymbol{R}$ can be obtained

$$\begin{aligned} f(\boldsymbol{\tau}, \boldsymbol{R}|\boldsymbol{Z}) &\propto \prod_{k=1}^{K} f(z_k|\boldsymbol{R}, \tau_k; H_0) f(\tau_k) f(\boldsymbol{R}) \\ &\propto |\boldsymbol{R}|^{-(\upsilon+N+K)} \mathrm{etr}\left\{ -\upsilon \boldsymbol{R}^{-1} \boldsymbol{\Sigma} \right\} \\ &\quad \times \prod_{k=1}^{K} \tau_k^{-(3/2+N)} \exp\left\{ -\left[\frac{\eta\tau_k}{2\mu} + \frac{q_k}{\tau_k} \right] \right\} \end{aligned} \tag{18}$$

where $\boldsymbol{Z} = [z_1, z_2, \ldots, z_K]$ and $q_k = \mu\eta/2 + z_k^H \boldsymbol{R}^{-1} z_k$, $k = 1, \ldots, K$. Exploiting the derivative of the logarithm of $f(\boldsymbol{\tau}, \boldsymbol{R}|\boldsymbol{Z})$ with respect to τ_k, $k = 1, 2, \ldots, K$, and setting it to zero, we get the MAP estimate of τ_k

$$\hat{\tau}_k^{\mathrm{MAP}} = \frac{\mu}{\eta}\left[-(N + 3/2) + \sqrt{(N + 3/2)^2 + \frac{2\eta}{\mu}q_k} \right]. \tag{19}$$

Substituting $\hat{\tau}_k^{\mathrm{MAP}}$ and $\hat{\upsilon}$ into (18), the derivative of the log-likelihood function with respect to $\boldsymbol{R}$ can be written as

$$\begin{aligned} &\frac{\partial \ln f(\hat{\boldsymbol{\tau}}, \boldsymbol{R}|\boldsymbol{Z})}{\partial \boldsymbol{R}} \\ &= -(\hat{\upsilon} + N + K)(\boldsymbol{R}^{\mathrm{T}})^{-1} + \hat{\upsilon}(\boldsymbol{R}^{\mathrm{T}})^{-1} \boldsymbol{\Sigma}^{\mathrm{T}} (\boldsymbol{R}^{\mathrm{T}})^{-1} \\ &\quad + \sum_{k=1}^{K} \left\{ -\left[\frac{N + \frac{3}{2}}{\hat{\tau}_k^{\mathrm{MAP}}} + \frac{\eta}{2\mu} - \frac{q_k}{\left(\hat{\tau}_k^{\mathrm{MAP}}\right)^2} \right] \right. \\ &\quad \left. \times \frac{\partial \hat{\tau}_k^{\mathrm{MAP}}}{\partial \boldsymbol{R}} - \left(\hat{\tau}_k^{\mathrm{MAP}}\right)^{-1} \frac{\partial q_k}{\partial \boldsymbol{R}} \right\}. \end{aligned} \tag{20}$$

The derivative of q_k with respect to $\boldsymbol{R}$ can be derived as

$$\frac{\partial q_k}{\partial \boldsymbol{R}} = -(\boldsymbol{R}^{\mathrm{T}})^{-1} (z_k z_k^H)^{\mathrm{T}} (\boldsymbol{R}^{\mathrm{T}})^{-1}. \tag{21}$$

From (19), the derivative of $\hat{\tau}_k^{\mathrm{MAP}}$ with respect to $\boldsymbol{R}$ can be given by

$$\frac{\partial \hat{\tau}_k^{\mathrm{MAP}}}{\partial \boldsymbol{R}} = \left[(N+3/2)^2 + \frac{2\eta}{\mu} q_k\right]^{-1/2} \frac{\partial q_k}{\partial \boldsymbol{R}}. \tag{22}$$

Substituting (21) and (22) into (20) and setting the result to zero, after some algebraic operation we can get

$$\begin{aligned}\boldsymbol{R} = {} & \frac{\hat{\upsilon}}{\hat{\upsilon}+N+K}\boldsymbol{\Sigma} + \frac{1}{\hat{\upsilon}+N+K} \\ & \times \sum_{k=1}^{K} \left\{ \left[\frac{N+3/2}{\hat{\tau}_k^{\mathrm{MAP}}} + \frac{\eta}{2\mu} - \frac{q_k}{\left(\hat{\tau}_k^{\mathrm{MAP}}\right)^2} \right] \right. \\ & \times \left[\left(N+\frac{3}{2}\right)^2 + \frac{2\eta}{\mu}\left(\frac{\mu\eta}{2} + \boldsymbol{z}_k^H \boldsymbol{R}^{-1} \boldsymbol{z}_k\right) \right]^{-1/2} \\ & \left. + \left(\hat{\tau}_k^{\mathrm{MAP}}\right)^{-1} \right\} \boldsymbol{z}_k \boldsymbol{z}_k^H. \end{aligned} \tag{23}$$

From (23), we can find $\boldsymbol{R} = f(\boldsymbol{R}, \boldsymbol{Z})$ and it can be solved via an iterative procedure $\boldsymbol{R}^{(n+1)} = f(\boldsymbol{R}^{(n)}, \boldsymbol{Z})$. The initial matrix $\boldsymbol{R}^{(0)}$ can be set to be an identity matrix or the NSCM estimate. To ensure $\mathrm{tr}\{\boldsymbol{R}^{(n+1)}\} = N$, we constrain the estimate after each iteration, i.e., $\boldsymbol{R}^{(n+1)} = N/\mathrm{tr}\{\boldsymbol{R}^{(n+1)}\}\boldsymbol{R}^{(n+1)}$, where $\mathrm{tr}\{\cdot\}$ denotes the trace of a matrix. After iterative computation, the final MAP estimate $\hat{\boldsymbol{R}}_{\mathrm{MAP}}$ of $\boldsymbol{R}$ can be obtained. It is highlighted that the MAP estimate in (23) is suitable for the estimation of $\boldsymbol{R}$ of CG-IG clutter, which differs from other types of clutter, such as the Gaussian clutter and the K-distributed clutter.

Substituting $\hat{\boldsymbol{R}}_{\mathrm{MAP}}$ into (14), an adaptive coherent detector called the generalized likelihood ratio test detector with training samples and prior information (GLRTD-TSPI) is obtained

$$(N+3/2)\ln\left(\frac{\hat{\tau}_0}{\hat{\tau}_1}\right) + \frac{\eta(\hat{\tau}_0 - \hat{\tau}_1)}{2\mu} + \frac{\hat{q}_0}{\hat{\tau}_0} - \frac{\hat{q}_1}{\hat{\tau}_1} \underset{H_0}{\overset{H_1}{\gtrless}} \gamma' \tag{24}$$

where $\hat{q}_0 = \mu\eta/2 + \boldsymbol{z}^H \hat{\boldsymbol{R}}_{\mathrm{MAP}}^{-1} \boldsymbol{z}$ and $\hat{q}_1 = \mu\eta/2 + \boldsymbol{z}^H \hat{\boldsymbol{R}}_{\mathrm{MAP}}^{-1} \boldsymbol{z} - |\boldsymbol{p}^H \hat{\boldsymbol{R}}_{\mathrm{MAP}}^{-1} \boldsymbol{z}|^2 (\boldsymbol{p}^H \hat{\boldsymbol{R}}_{\mathrm{MAP}}^{-1} \boldsymbol{p})^{-1}$.

IV. Performance Assessment

In this section, we evaluate the performance of the proposed GLRTD-TSPI. GLRT-IG in [15] and BGLRTD-NSD in [14] are considered as its competitors. For the simulated clutter data, the random speckle covariance matrix $\boldsymbol{R}$ is generated via the inverse complex Wishart distribution with the matrix $\boldsymbol{\Sigma}$ whose elements are given by $[\boldsymbol{\Sigma}]_{i,j} = \rho^{|i-j|}$, $1 \le i, j \le N$. Other clutter parameters are set as $N = 8$, $\mu = 1$, $\rho = 0.95$, $\upsilon = 16$, $\upsilon_l = N+1$, and $\upsilon_u = 3N$. The target parameter f_d is set as $f_d = 0.3$. The probability of false alarm (Pfa) is $P_{fa} = 10^{-4}$, and the detection thresholds are obtained via $100/P_{fa}$ independent Monte Carlo experiments. The average signal clutter ratio (A-SCR) is defined as

$$\text{A-SCR} = 10\log_{10}\frac{|\alpha^2|\mathbf{p}^H\mathbf{p}}{N\mu}(\text{dB}). \tag{25}$$

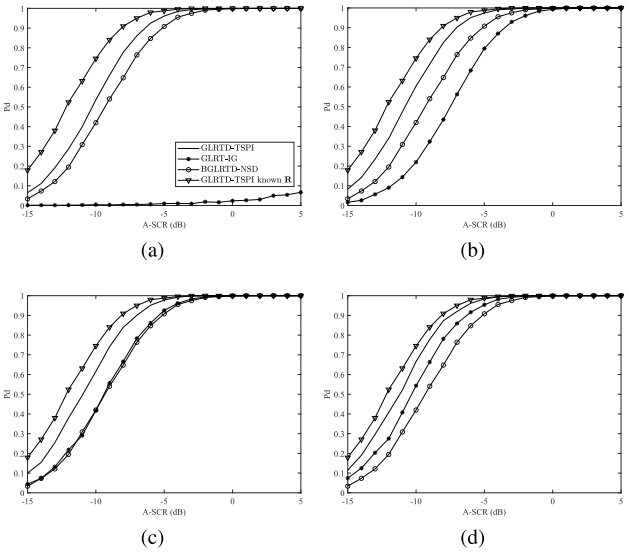

Fig. 1. Performance comparisons using simulated data and assuming $\eta = 2$, $\mu = 1$, $\rho = 0.95$, and $\upsilon = 16$. (a) $K = 8$, (b) $K = 16$, (c) $K = 24$, and (d) $K = 32$.

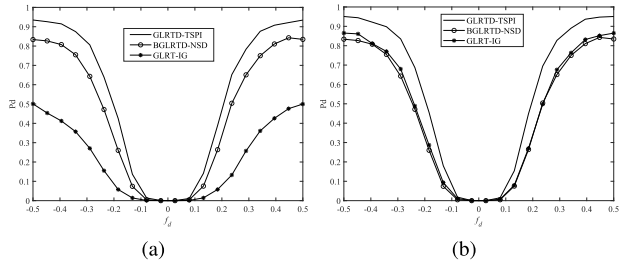

Fig. 2. Performance comparisons for different f_ds with $\eta = 2$, $\mu = 1$, $\rho = 0.95$, $\upsilon = 16$, and A-SCR = -8 dB. (a) $K = 14$ and (b) $K = 24$.

Fig. 1 shows the probability of detection (Pd) curves of three detectors for different numbers of training samples when the simulated data are used. GLRT-IG uses the CAML estimator to estimate the speckle covariance matrix, and BGLRT-NSD adopts $\boldsymbol{\Sigma}$ as the prior matrix. The iteration number of both the CAML estimator and the proposed estimator in (23) is set to 3. As seen, GLRT-IG suffers much performance loss compared with the proposed GLRTD-TSPI and the BGLRTD-NSD in Fig. 1(a) and (b). Contrarily, the Pd of GLRT-IG increases with the increase in the number of training samples, and finally exceeds the Pd of BGLRTD-NSD in Fig. 1(d). On the whole, the proposed GLRTD-TSPI performs the best performance than GLRT-IG and BGLRTD-NSD for different numbers of training samples. The reason is that the proposed GLRTD-TSPI jointly uses the prior information and the training samples to improve the detection performance.

Next, the influence of the target Doppler frequency on three detectors is studied in Fig. 2. As observed in Fig. 2(a) and (b), the Pd gradually decreases for all the detectors as f_d approaches the endo-clutter region. The target needs to compete with most of the clutter's energy when it appears in the endo-clutter region, so the detection performance degrades. Similarly, the proposed GLRTD-TSPI has the highest Pd among three detectors.

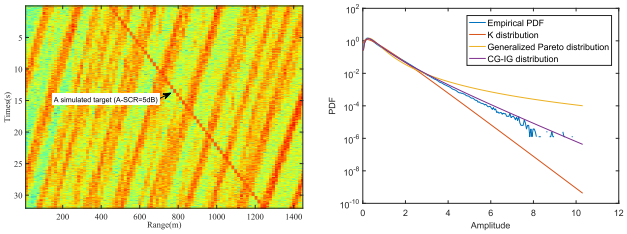

(a) (b)

Fig. 3. Analysis of clutter amplitudes. (a) Time-range power of real clutter plus simulated target and (b) amplitude fitting results.

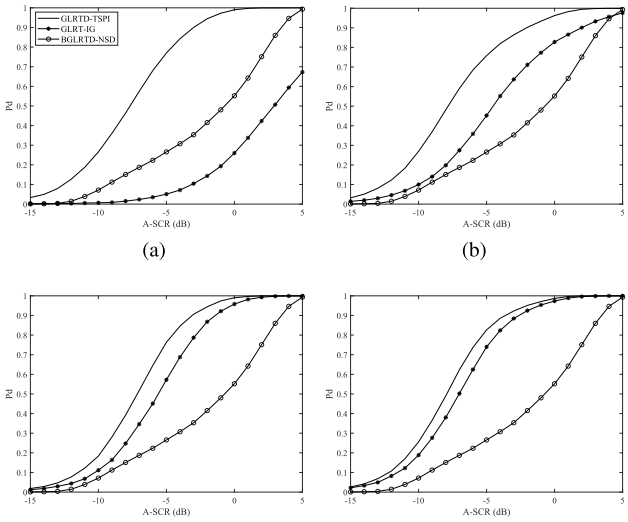

(a) (b) (c) (d)

Fig. 4. Performance comparisons using the measured sea clutter plus the simulated target with $\eta = 0.53$ and $\mu = 0.67$. (a) $K = 10$, (b) $K = 16$, (c) $K = 24$, and (d) $K = 32$.

Finally, the detection performance of three detectors is carried out via the South Africa measured sea clutter data [18]. The carrier frequency of the experiment radar is 9 GHz, the pulse repetition frequency is 5 kHz, and the range resolution is 15 m. The TFC15_005 data are adopted as the real sea clutter data. For the selected data, the wind speed is about 7.8 m/s, and the significant wave height is about 3.1 m. First, we investigate the amplitude statistical property of the real sea clutter in Fig. 3. From Fig. 3(a), we can see that the amplitudes of sea clutter present the large fluctuations. In Fig. 3(b), the empirical PDF and the fitting results show that CG-IG distribution has the best fitting performance for the main part and the tailing part than other distributions. Therefore, the inverse Gaussian distribution is suitable to model the texture component of the selected sea clutter data. In Fig. 4, the Pd curves of three detectors are shown for different numbers of training samples. The prior matrix $\mathbf{\Sigma}$ can be obtained using the same procedure in [14]. As observed in Fig. 4, GLRTD-TSPI outperforms GLRT-IG and BGLRTD-NSD for different numbers of training samples, especially when the training samples are starved.

V. Conclusion

In this letter, we studied the adaptive target detection problem in the training-sample-starved sea clutter environment. Based on the 2S-GLRT and MAP estimates of the clutter texture and the speckle covariance matrix, we proposed GLRTD-TSPI to detect radar targets embedded in sea clutter environments. The performance comparisons using the simulated and measured data show that GLRTD-TSPI performs the best for different situations compared with BGLRTD-NSD and GLRT-IG, especially when the training samples are starved.

References

[1] F. Gini, M. V. Greco, M. Diani, and L. Verrazzani, "Performance analysis of two adaptive radar detectors against non-Gaussian real sea clutter data," *IEEE Trans. Aerosp. Electron. Syst.*, vol. 36, no. 4, pp. 1429–1439, Oct. 2000.

[2] K. D. Ward, "Compound representation of high resolution sea clutter," *Electron. Lett.*, vol. 17, no. 16, pp. 561–563, Aug. 1981.

[3] E. Conte, A. De Maio, and C. Galdi, "Statistical analysis of real clutter at different range resolutions," *IEEE Trans. Aerosp. Electron. Syst.*, vol. 40, no. 3, pp. 903–918, Jul. 2004.

[4] L. Rosenberg and S. Bocquet, "Application of the Pareto plus noise distribution to medium grazing angle sea-clutter," *IEEE J. Sel. Topics Appl. Earth Observ. Remote Sens.*, vol. 8, no. 1, pp. 255–261, Jan. 2015.

[5] E. Ollila, D. E. Tyler, V. Koivunen, and H. V. Poor, "Compound-Gaussian clutter modeling with an inverse Gaussian texture distribution," *IEEE Signal Process. Lett.*, vol. 19, no. 12, pp. 876–879, Dec. 2012.

[6] A. Mezache, F. Soltani, M. Sahed, and I. Chalabi, "Model for non-Rayleigh clutter amplitudes using compound inverse Gaussian distribution: An experimental analysis," *IEEE Trans. Aerosp. Electron. Syst.*, vol. 51, no. 1, pp. 142–153, Jan. 2015.

[7] E. J. Kelly, "An adaptive detection algorithm," *IEEE Trans. Aerosp. Electron. Syst.*, vol. AES-22, no. 1, pp. 115–127, Mar. 1986.

[8] E. Conte, M. Lops, and G. Ricci, "Adaptive matched filter detection in spherically invariant noise," *IEEE Signal Process. Lett.*, vol. 3, no. 8, pp. 248–250, Aug. 1996.

[9] F. Gini and M. S. Greco, "Covariance matrix estimation for CFAR detection in correlated heavy tailed clutter," *Signal Process.*, vol. 82, no. 12, pp. 1847–1859, Dec. 2002.

[10] O. Besson, J.-Y. Tourneret, and S. Bidon, "Knowledge-aided Bayesian detection in heterogeneous environments," *IEEE Signal Process. Lett.*, vol. 14, no. 5, pp. 355–358, May 2007.

[11] F. Bandiera, O. Besson, and G. Ricci, "Adaptive detection of distributed targets in compound-Gaussian noise without secondary data: A Bayesian approach," *IEEE Trans. Signal Process.*, vol. 59, no. 12, pp. 5698–5708, Dec. 2011.

[12] L. Kong, N. Li, G. Cui, H. Yang, and Q. H. Liu, "Adaptive Bayesian detection for multiple-input multiple-output radar in compound-Gaussian clutter with random texture," *IET Radar, Sonar Navigat.*, vol. 10, no. 4, pp. 689–698, Apr. 2016.

[13] Y. Gao, H. Li, and B. Himed, "Knowledge-aided range-spread target detection for distributed MIMO radar in nonhomogeneous environments," *IEEE Trans. Signal Process.*, vol. 65, no. 3, pp. 617–627, Feb. 2017.

[14] J. Xue, S. Xu, and P. Shui, "Knowledge-based target detection in compound Gaussian clutter with inverse Gaussian texture," *Digit. Signal Process.*, vol. 95, Dec. 2019, Art. no. 102590.

[15] S. Chen, L. Kong, and J. Yang, "Adaptive detection in compound-Gaussian clutter with inverse Gaussian texture," *Prog. Electromagn. Res. M*, vol. 28, pp. 157–167, 2013.

[16] J. R. Guerci and E. J. Baranoski, "Knowledge-aided adaptive radar at DARPA: An overview," *IEEE Signal Process. Mag.*, vol. 23, no. 1, pp. 41–50, Jan. 2006.

[17] J. Liu, J. Han, Z.-J. Zhang, and J. Li, "Bayesian detection for MIMO radar in Gaussian clutter," *IEEE Trans. Signal Process.*, vol. 66, no. 24, pp. 6549–6559, Dec. 2018.

[18] P. L. Herselman and C. J. Baker, "Analysis of calibrated sea clutter and boat reflectivity data at C- and X-band in South African coastal waters," in *Proc. IET Int. Conf. Radar Syst.*, 2007, pp. 140–144.